Advances in Water Resources 61 (2013) 42–50

Contents lists available at ScienceDirect

Advances in Water Resources

journal homepage: www.elsevier.com/locate/advwatres

Spatial downscaling of TRMM precipitation data based on the orographical effect and meteorological conditions in a mountainous area

Jian Fang [a,c], Juan Du [a,b,c,*], Wei Xu [a,b,c], Peijun Shi [a,b,c], Man Li [a,c], Xiaodong Ming [a,c]

[a] State Key Laboratory of Earth Surface Processes and Resource Ecology, Beijing Normal University, Beijing 100875, China
[b] Key Laboratory of Environmental Change and Natural Disaster, Ministry of Education of China, Beijing Normal University, Beijing 100875, China
[c] Academy of Disaster Reduction and Emergency Management, Ministry of Civil Affairs & Ministry of Education, P.R., Beijing 100875, China

ARTICLE INFO

Article history:
Received 4 April 2013
Received in revised form 5 July 2013
Accepted 21 August 2013
Available online 28 August 2013

Keywords:
Spatial downscaling
TRMM
Extreme rainfall events
Orographical effect
Pre-storm conditions

ABSTRACT

The lack of high resolution precipitation data has posed great challenges to the study and management of extreme rainfall events. Satellite-based rainfall products with large areal coverage provide a potential alternative source of data where in situ measurements are not available. However, the mismatch in scale between these products and model requirements has limited their application and demonstrates that satellite data must be downscaled before being used. This study developed a statistical spatial downscaling scheme based on the relationships between precipitation and related environmental factors such as local topography and pre-storm meteorological conditions. The method was applied to disaggregate the Tropical Rainfall Measuring Mission (TRMM) 3B42 products, which have a resolution of 0.25° × 0.25°, to 1 × 1 km gridded rainfall fields. The TRMM datasets in accord with six rainstorm events in the Xiao River basin were used to validate the effectiveness of this approach. The downscaled precipitation data were compared with ground observations and exhibited good agreement with r^2 values ranging from 0.612 to 0.838. In addition, the proposed approach provided better results than the conventional spline and kriging interpolation methods, indicating its promise in the management of extreme rainfall events. The uncertainties in the final results and the implications for further study were discussed, and the needs for additional rigorous investigations of the rainfall physical process prior to institutionalizing the use of satellite data were highlighted.

1. Introduction

Extreme rainfall events are of increasing concern to both the scientific and management communities [1,2] because of the observed and projected higher frequency of such events [3,4] and the occurrence of several disastrous floods in Asia and Europe in recent years [5]. In this context, linking atmospheric and surface processes and assessing the impacts of extreme precipitation events are critical steps toward effective risk reduction and climate change adaptation.

However, ongoing research in this field is hindered by several impediments. In addition to model deficiencies, the lack of high-quality precipitation data is just as challenging [6]. Given the small-scale variability of precipitation and the sparseness of observation networks, conventional in situ point measurements cannot effectively reflect the spatial variability of precipitation and are inherently weak in forcing hydrological models, which perform better with areal precipitation [7]. In the past decades, several satellite-based precipitation products have been developed globally, including the Global Precipitation Climatology Project [8], the Precipitation Estimation from Remotely Sensed Information using Artificial Neural Networks [9] and the Tropical Rainfall Measuring Mission [10]. These products provide a promising alternative data source for hydrological applications with high spatial–temporal resolution and large areal coverage [11]. However, the existing gap in scale between the relatively low spatial resolution satellite precipitation data and the high resolution required by hydrological models has limited the wide application of these products [12]. Therefore, spatial downscaling of remote sensing precipitation data is necessary before they are used to investigate the hydrological response to extreme rainfall events.

In essence, spatial downscaling attempts to capture the subgrid heterogeneity while preserving the characteristics at the original scale. The key concept is scale invariance or relating the properties of the physical process at different scales [13]. Several downscaling methods have been developed based on different hypotheses and for various applications. One class of these approaches highlights the orographical effect on spatial variability of rainfall and incorporates topographical features into the downscaling scheme or interpolation process. For example, Prudhomme and Reed [14] developed a regression equation that relates the

* Corresponding author at: State Key Laboratory of Earth Surface Processes and Resource Ecology, Beijing Normal University, Beijing 100875, China. Tel.: +86 10 58808661.
E-mail address: juan.du@bnu.edu.cn (J. Du).

0309-1708/$ - see front matter © 2013 Elsevier Ltd. All rights reserved.
http://dx.doi.org/10.1016/j.advwatres.2013.08.011

precipitation index to topographical variables and used it with the modified residual kriging method to map extreme rainfall in the mountainous region of Scotland. Jia et al. [15] downscaled the TRMM 3B43 derived annual precipitation data to 1×1 km fields in the Qaidam Basin of China based on the relationships among precipitation, topography and vegetation. While the mechanism of the orographical effect is complex and depends on the interaction between local topography and atmospheric flows [16]; it requires careful examination and proper representation. In addition, the topographical influence is static and not sufficient to explain the spatial variation of precipitation. Another class of downscaling approaches is based on the multi-scaling spectral properties of rainfall fields assuming that the statistical characteristics of the rainfall fields at different scales can be linked with a parameter that is scale-invariant or has a specific structure related to a physical variable governing the rainfall dynamics [17]. Typical examples of these approaches include the Haar wavelet transform methods [13,18,19] and the fractal and stochastic cascade-based multifractal methods [20,21]. However, in the scaling-based approaches, the relationships between atmospheric dynamics and precipitation statistics at all spatial scales are weak and implicit, which limits their use in short duration storm prediction [22]. In addition, the scaling properties exhibit strong geographical and seasonal variability, which complicates the development of these models [12].

The key questions in physical process-oriented downscaling schemes are what the main factors that govern the spatial variability of rainfall are and how this information can be used to capture the sub-grid heterogeneity of precipitation. The orographical effect is believed to be an important mechanism that controls the spatial variability of precipitation in mountainous areas. Meanwhile, in the case of convective systems, pre-storm meteorological conditions such as temperature and humidity, also have large influences on small-scale moisture content and the system stability [23] and thus determine the intensity of local convective rains.

In this study, we developed a statistical downscaling method that combines the orographical effect and pre-storm conditions and disaggregated the TRMM 3B42 precipitation products to 1×1 km fields for six rainstorm events in a medium-size basin in China. First, the relationships among precipitation, topographical factors and pre-storm conditions were examined, and a multivariate regression model was established at the original scale. The model was then transferred to the target scale and combined with the stochastically interpolated residuals to derive the precipitation field at the desired resolution. Finally, the results were validated and discussed for future research.

2. Methodology

2.1. Study area

The study area is the Xiao River basin, which is a medium-size catchment with a total area of 12,099 km^2 and located in the southeast part of Hunan Province in central and southern China (see Fig. 1). The Xiao River originates in the mountainous area in the southeast part of the basin and runs from southeast to northwest into the upper reaches of the Xiangjiang River, a tributary of the Yangtze River. Hilly areas make up 49.45% of the total land area in the Xiao River basin, and the elevations range from 88 to 1980 m. High mountains are located in the middle and southern areas, and relatively flat valleys lie between the mountains. The annual precipitation of the Xiao River basin varies from 1200 to 1900 mm and decreases from south to north and from the mountainous areas to the plains. Influenced by the East Asia Monsoon, water vapor mainly comes from the sea to the southeast, and precipitation is concentrated in the summer and autumn. The complex topography and the vapor-rich synoptic system (monsoon and occasional typhoons) lead to frequent extreme rainfall events and make the area prone to floods (especially flash floods in mountainous area) that cause economic loss of several million RMB every year.

2.2. Datasets

The satellite-based precipitation data used in this study are from the Tropical Rainfall Measuring Mission (TRMM), a joint project launched by NASA and the Japanese space agency JAXA. TRMM carries several precipitation measuring instruments, such as the Precipitation Radar (PR), the TRMM Microwave Imager (TMI) and the Visible & Infrared Scanner (VIRS). The information from these instruments is processed with retrieval algorithms to generate precipitation estimates at a quasi-global scale [10]. TRMM provides a range of products with different processing algorithms among which the 3-hourly 3B42 V7 dataset with a spatial resolution of 0.25° was used in this study. The dataset is a multi-satellite precipitation product that is calibrated with the TRMM Combined Instrument (TCI) estimates and gauge data provided by the Global Precipitation Climatological Center and the Climate Assessment and Monitoring System. Six rainstorm events were selected in this study (see Table 1). Consecutive files of the original 3-hourly 3B42 data corresponding to each rainstorm event were accumulated to obtain the event-based precipitation data.

The Digital Elevation Model (DEM) data are obtained from the Shuttle Radar Topography Mission (SRTM) project, which is sponsored by the National Geospatial-Intelligence Agency (NGA) and NASA. Launched on February 2000, the SRTM provides digital topographical data with spatial coverage of 56°S to 60°N and a resolution of 1 arc second (approximately 30 m). While the 1 s data are released for the United States only, the composite 3-arc-second data are available for other regions and were therefore used in this study (http://srtm.csi.cgiar.org/).

The meteorological data are collected from the local meteorological agency and include precipitation, pre-storm maximum temperature and humidity from eight local meteorological stations (see Fig. 1). The TRMM 3B42 data were firstly calibrated with the ground-observed precipitation from the available stations. As in Sawunyama [24] and Jia et al. [15], the non-linear optimized relation between the data from these two sources was examined, and a power function was employed to correct the satellite-based precipitation data for each event. Table 1 shows the calibration results.

2.3. Method

The method used in this study is based on the assumption that the spatial variability of precipitation is well captured by the TRMM products and can be explained by local topography and the pre-storm meteorological conditions. Antecedent maximum temperature and average humidity are the two primary indices for pre-storm conditions and are obtained through the interpolation of ground-based observations across various scales. The orographical effect can be represented in three different factors: the elevation of the target pixel, the angle between the slope aspect and the prevailing wind direction, and the topographical roughness in the direction of the dominant airflow. The variable of topographical roughness was adopted from Prudhomme [25] and calculated as the weighted average of ups and downs in elevation from the current pixel to the border of the study area in the direction of dominant airflow. The formula for topographical roughness is as follows:

$$updown_i = \frac{\sum_{t=1}^{N} dist_{(N-t+1)} \times elev\_dif_t}{\sum_{t=1}^{N} dist_t} \quad (1)$$

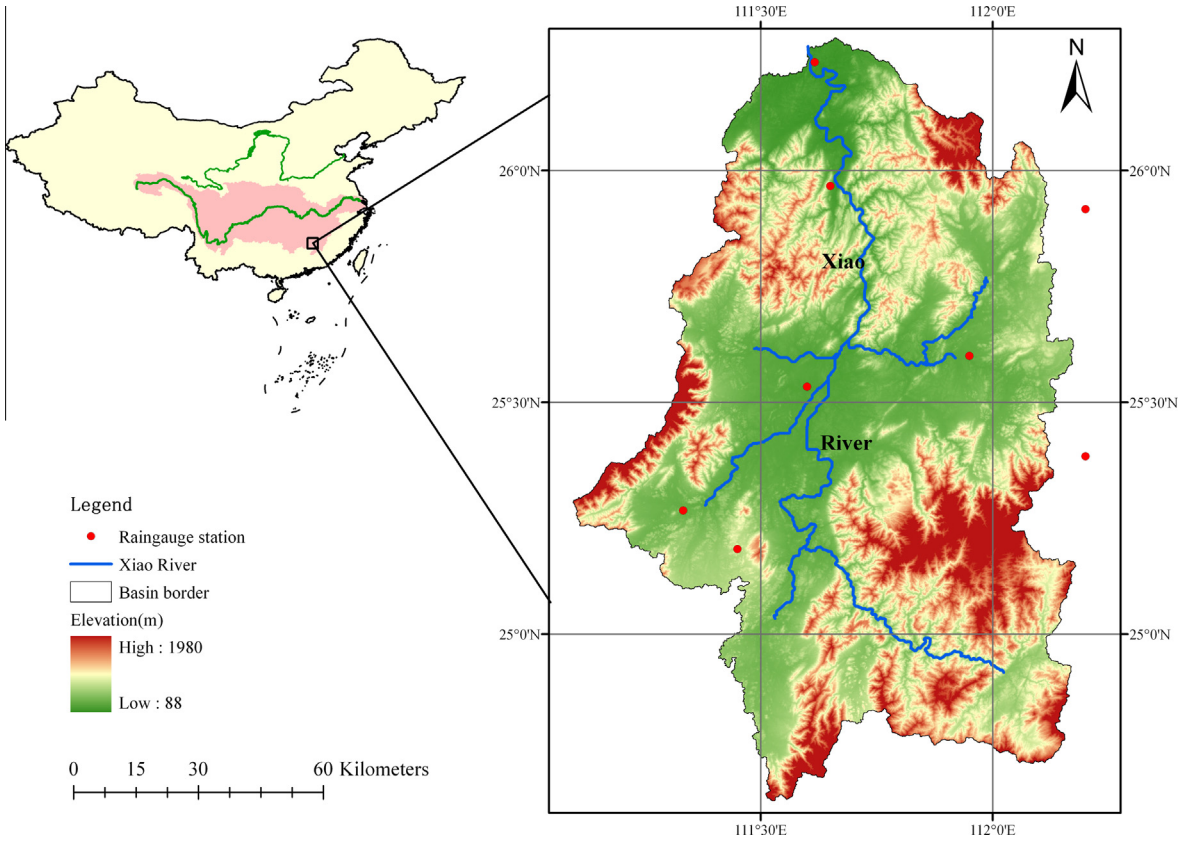

Fig. 1. The location and topography of the Xiao River basin.

Table 1
The six selected rainstorm events and their calibration.

ID	Date	Spatial maximum precipitation (mm)	Spatial average precipitation (mm)	Coefficient of variation	Calibration *R*-square	Calibration RMSE
e1	2001/6/11–2001/6/13	218.16	126.38	0.417	0.827	63.796
e2	2002/5/8–2002/5/9	132.20	57.66	0.427	0.646	31.309
e3	2002/5/14–2002/5/14	99.25	53.42	0.366	0.655	16.580
e4	2006/5/25–2006/5/26	137.83	73.12	0.419	0.519	51.975
e5	2006/7/15–2006/7/16	181.82	152.25	0.113	0.319	38.207
e6	2010/6/1–2010/6/2	74.33	59.43	0.216	0.591	34.815

$$roughness = \frac{\sum_{i=1}^{9} \cos\alpha_i \times updown_i}{\sum_{i=1}^{9} \cos\alpha_i} \quad (2)$$

where $updown_i$ denotes the elevation ups and downs in sub-direction i; there are nine sub-directions centered at the prevailing wind direction; $dist_t$ is the distance from the current operating pixel to pixel t in the given sub-direction; $elev\_dif_t$ denotes the absolute difference in elevation between pixel t and pixel $(t+1)$; N is the number of pixels in each sub-direction; and a_i is the angle between sub-direction i and the prevailing wind direction.

As described in Fig. 2, the relationships among precipitation, the topographical factors and the pre-storm meteorological conditions for each event were first examined at the original scale of 0.25°, and a multivariate linear regression model was constructed. The residuals were then calculated as the differences between the original TRMM 3B42 data and predicted values from the model. The residuals are interpreted as the natural random variations of precipitation that are not represented by the model and were interpolated to a 1 km resolution using the spline interpolator. The predicted values of precipitation at the target scale of 1 km were then calculated using the previously constructed regression model and detailed information of the explanatory variables. Finally, the downscaling result was obtained by combining the interpolated residuals and the predicted precipitation.

To validate the downscaling approach, the results were compared with the observations from the eight raingauge stations. Conventional spline and kriging interpolation methods were also implemented to provide a comparison with the proposed approach. Three indices were chosen as comparison criteria: the coefficient of determination (r^2), the bias (B) and the root mean square error (RMSE). The latter two indices are calculated as follows:

$$B = \frac{\sum_{i=1}^{n} p_{mi}}{\sum_{i=1}^{n} p_{oi}} - 1 \quad (3)$$

$$\mathrm{RMSE} = \left(\sum_{i=1}^{n} (p_{mi} - p_{oi})^2 \Big/ n \right)^{1/2} \quad (4)$$

where n is the total number of stations; i is the index of the station; p_{mi} is the model downscaled precipitation of station i; and p_{oi} is the observed precipitation of station i.

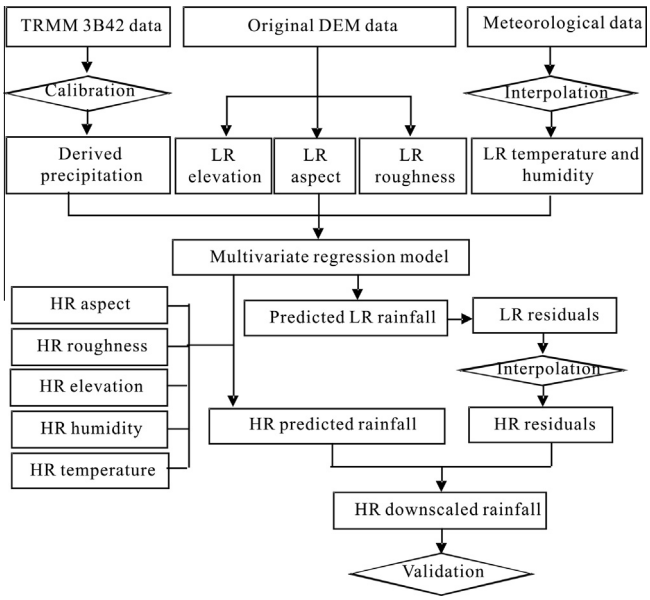

Fig. 2. Schematic overview of the downscaling method. Note: LR represents low resolution and refers to a resolution of 0.25° × 0.25°, while HR represents high resolution and refers to the 1 × 1 km resolution in this study.

3. Results

3.1. Univariate regression analysis

To investigate the impacts of topographical and meteorological factors on the spatial variability of severe convective rainfall, the relationships between precipitation and the explanatory variables were first examined individually through univariate regression analysis at the solved scale of 0.25°. The original 90 m-resolution DEM data were upscaled to 0.25° and then used to calculate the topographical variables of elevation, slope aspect and topographical roughness for each pixel. The meteorological variables of pre-storm temperature and humidity at the 0.25° resolution were obtained through spatial interpolation of the ground-observed data.

The results are presented in Table 2 and show the percentage of variance in precipitation that is explained by each variable (r^2). Overall, the pre-storm meteorological variables had greater effects than the topographical variables. The coefficients of determination (r^2) of the meteorological variables varied from 0.716 to 0.003, and almost all were significant at the level of $p < 0.1$, while the highest r^2 value of the topographical variables was 0.292, and many did not pass the significance test. Specifically, among the topographical variables, the angle between slope aspect and the prevailing wind direction (aspect_angle) gave better results than the single aspect variable (aspect_catg). Higher r^2 values were found for the aspect angle variable in four of the six events; the remaining two were not significant at the $p < 0.1$ level, and the r^2 values were so low that both of the variables can be ignored in explaining the variations of precipitation. Similar results were also found for the variables of topographical roughness and pixel elevation. The variance in precipitation explained by topographical roughness was at least 165% greater than that explained by the elevation.

3.2. Multivariate regression analysis

A multivariate regression analysis with all of the significant variables was carried out for each event to find the best-fitting relationship between precipitation and the local environmental factors. As shown in Section 3.1, the angle between slope aspect and wind direction performed better than only the aspect in explaining the variation of precipitation; thus it would replace the slope aspect variable in the multivariate regression model. With regard to elevation-related variables, although topographical roughness explained more than the pixel elevation, both of them were incorporated into the model because they reflect the influences of elevation on precipitation from different perspectives. All five variables (elevation, aspect angle, roughness, temperature and humidity) were included in the model in the initial step to ensure that all of the valuable information would be retained. The variables that failed to pass the significance test (at the $p < 0.05$ level) were then rejected, and the final regression model for each event was constructed.

Based on the regression models, the predicted precipitation was calculated and compared with the calibrated TRMM data at the 0.25° resolution. Fig. 3 shows the results of the

Table 2
The results of regression analysis between precipitation and explanatory topographical and meteorological variables for the six events.

Event	Variable (acronym)	r^2	Event	Variable (acronym)	r^2
e1	aspect_catg (ASC)	0.001	e4	aspect_catg (ASC)	0.049
	aspect_angle (ASA)	0.021		aspect_angle (ASA)	0.047
	Roughness (RGH)	0.060		***Roughness (RGH)***	0.045
	Elevation (ELE)	0.008		***Elevation (ELE)***	0.017
	Temperature (TEM)	0.191**		***Temperature (TEM)***	0.054
	Humidity (HUM)	0.716**		***Humidity (HUM)***	0.306**
	Multivariate	0.841**		Multivariate	0.762**
e2	aspect_catg (ASC)	0.000	e5	aspect_catg (ASC)	0.011
	aspect_angle (ASA)	0.136**		aspect_angle (ASA)	0.079
	Roughness (RGH)	0.098*		***Roughness (RGH)***	0.175**
	Elevation (ELE)	0.025		***Elevation (ELE)***	0.016
	Temperature (TEM)	0.440**		***Temperature (TEM)***	0.003
	Humidity (HUM)	0.009		***Humidity (HUM)***	0.644**
	Multivariate	0.715**		Multivariate	0.742**
e3	aspect_catg (ASC)	0.001	e6	aspect_catg (ASC)	0.007
	aspect_angle (ASA)	0.292**		aspect_angle (ASA)	0.004
	Roughness (RGH)	0.099*		***Roughness (RGH)***	0.070
	Elevation (ELE)	0.011		***Elevation (ELE)***	0.001
	Temperature (TEM)	0.105*		***Temperature (TEM)***	0.080*
	Humidity (HUM)	0.328**		***Humidity (HUM)***	0.034
	Multivariate	0.483**		Multivariate	0.612**

Note: * indicates significance at a level of $p < 0.1$; ** indicates significance at a level of $p < 0.05$; the italic bold variables are selected in the multivariate regression model for each event.

multivariate regression models and scatter diagrams of the comparisons. All of the six models passed the significance test ($p < 0.05$) with r^2 values ranging from 0.483 to 0.841. The best fit was found in event e1, while event e3 was the least optimum. The model form and variables included in each model varied markedly among the different events. In event e3, only two of the five variables (aspect angle and humidity) were selected based on the significance test, while three or four variables could be used for the other five events. The significant differences among these models imply the complex dynamics of heavy rainfall events; different factors may interact with each other and contribute to the formation of intensive precipitation in complicated ways. In addition, temperature or humidity was used for events e2 and e3, respectively, and both of them were used for events e1, e4, e5 and e6. This supported the finding from Section 3.1 that the pre-storm meteorological conditions are more important than the influence of topography.

In most of the events, precipitation increased with elevation, temperature and humidity, which was manifested in events e5 and e6, while it decreased with aspect angle and topographical roughness, which was shown in events e2, e3 and events e5, e6, respectively. It is notable that models for some of the events disagreed with these findings, which reinforces the complex mechanisms of heavy rainfall events.

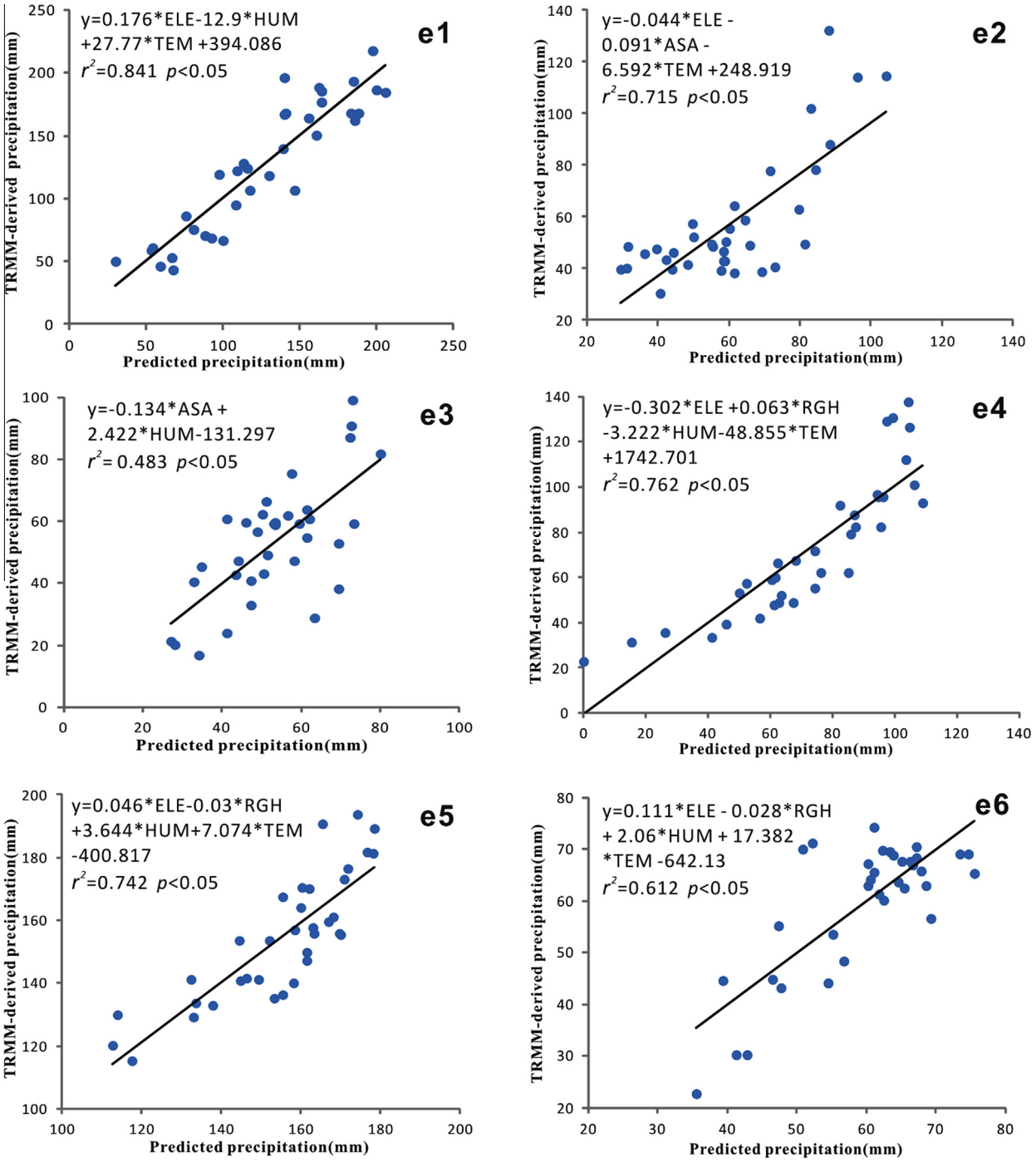

Fig. 3. Regression models and comparisons between predictive precipitation and TRMM derived precipitation for the six events.

3.3. Spatial downscaling process

This section uses event e1 as an example to illustrate the downscaling process. The 0.25° calibrated TRMM precipitation field is shown in Fig. 4a and indicates that precipitation in the south and southeast is much higher than that in the north, especially in the northwest part of the study area. Based on the multivariate regression model constructed at the 0.25° resolution and using the topographical and meteorological variables at the 1 km resolution, the 1 km precipitation was estimated by assuming that the same responses existed at the high resolution. Fig. 4b shows the results of the 1 km predicted precipitation. A similar pattern can be found with the 0.25° calibrated TRMM precipitation. The 0.25° predicted precipitation was subtracted from the original data to

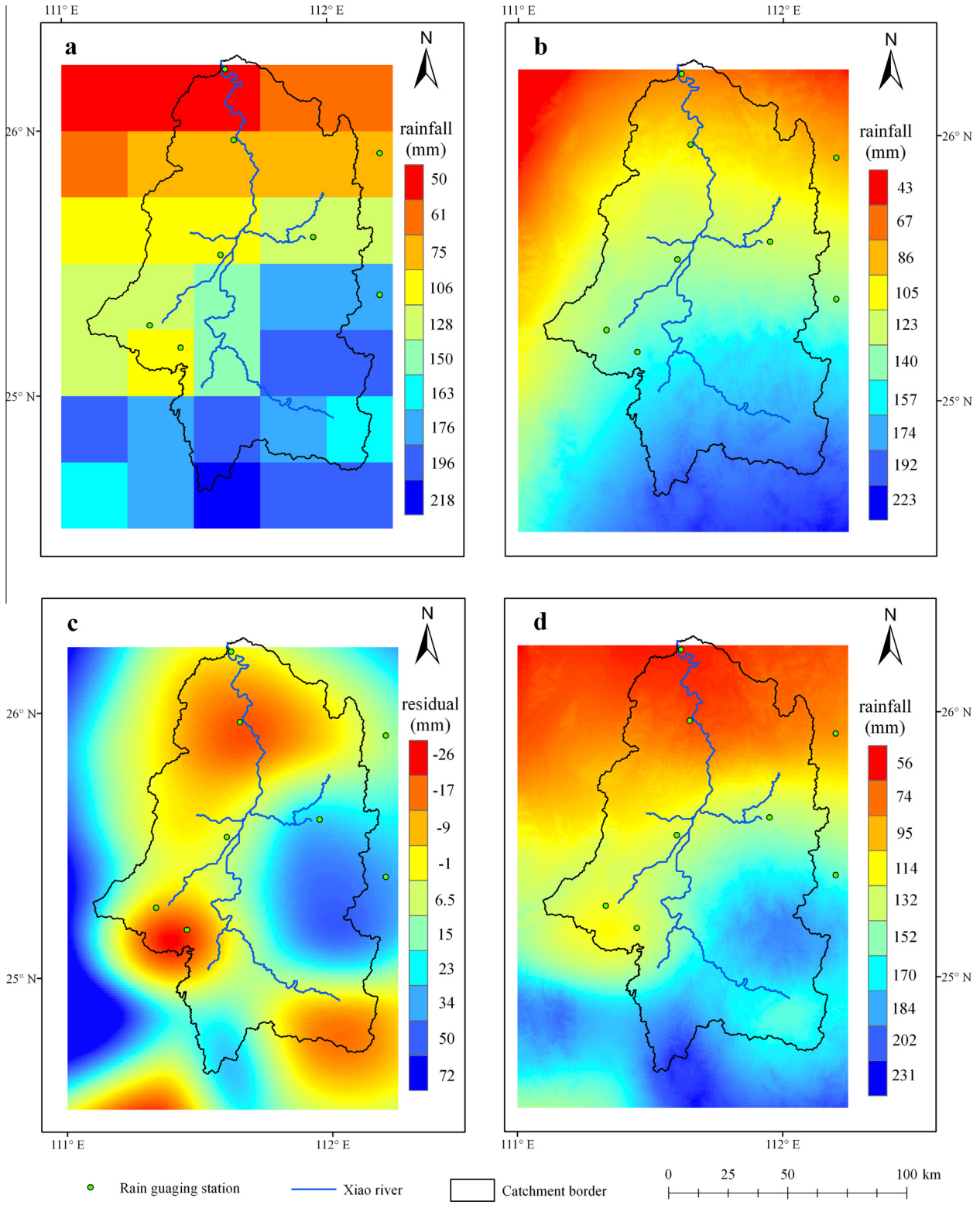

Fig. 4. Downscaling process for e1: (a) the calibrated TRMM 3B42 precipitation at 0.25° resolution; (b) the predictive precipitation at 1 km resolution; (c) the interpolated residuals at 1 km resolution; (d) the final downscaled result of precipitation at 1 km resolution.

Table 3
Validation of the downscaled results and the original TRMM 3B42 data for the six events.

Event	Coefficient of determination (r^2)		RMSE		Bias	
	Original	Downscaled	Original	Downscaled	Original	Downscaled
e1	0.7841	0.6680	63.7959	22.5505	−0.5973	−0.0314
e2	0.8735	0.8377	31.3094	15.3615	−0.4564	−0.1248
e3	0.5510	0.0443	16.5801	13.9196	0.2527	−0.0924
e4	0.3714	0.6984	51.9747	29.1682	0.5360	−0.2415
e5	0.4238	0.6122	38.2072	21.7870	−0.1275	0.0519
e6	0.4953	0.6301	34.8153	17.1373	−0.4772	0.0037

Table 4
Cross validation for conventional spline and kriging interpolation methods.

Event	Coefficient of determination (r^2)		RMSE		Bias	
	Spline	Kriging	Spline	Kriging	Spline	Kriging
e1	0.0790	0.0008	37.1831	39.5013	0.0654	0.0058
e2	0.1289	5.46E−05	31.6404	36.0122	−0.0744	0.0074
e3	0.3599	0.6639	19.0172	15.9461	0.0480	−0.0190
e4	0.3429	0.1545	35.7454	41.2124	−0.0233	0.0916
e5	0.0451	0.1540	45.1604	37.3523	0.0908	0.0026
e6	0.1354	0.5178	40.0527	34.0333	0.0686	−0.0225

obtain the residuals, which were subsequently interpolated to 1 km resolution using the spline interpolating approach. Some other interpolation methods such as IDW and kriging were also tried and little change in the final results could be observed with average relative change equaled to 4.84%, indicating weak sensitivity of final results on residuals. The interpolated result is shown in Fig. 4c with positive deviations in the outer part of the study area and negative biases in the interior. The final downscaled precipitation was produced by adding the interpolated residuals to the 1 km predicted precipitation obtained above. The final results of the downscaled precipitation field (Fig. 4d) resembled the original precipitation field (Fig. 4a); both showed decreasing precipitation from the southeast to the northwest. The result captured the spatial pattern of the original precipitation field well and restored it at a higher resolution.

3.4. Validation

The validation processes used to evaluate the efficiency of the proposed downscaling approach were all based on the comparison with ground-observed records using three criteria: the coefficient of determination (r^2), the root mean square error (RMSE) and the bias. Firstly, the final precipitation at the locations of the eight raingauge stations were extracted from the downscaled fields and compared with the station observations. Except for event e3, the downscaled results were characterized with r^2 values exceeding 0.6, indicating good agreement with the observed precipitation (Table 3). The RMSE values varied from 13.92 to 29.17 and were generally lower than one third of the mean precipitation for each event. The biases for four events (e1, e2, e3, e4) were less than 0, indicating underestimation of the precipitation, while precipitation were overestimated (positive biases) in events e5 and e6. The tendency of underestimation is related to the geographical location of the raingauge stations, which generally lie in the flat low lands at lower than average elevations.

It is notable that a better regression model does not necessarily give better downscaled results. The model fitting r^2 of event e1 (0.841) was the highest among the six events, while the validation r^2 ranked third (0.668); the validation r^2 of event e2 was the highest even though the model fitting r^2 was second lowest.

The original TRMM 3B42 precipitation data were also validated using the same procedure to provide a comparison with the downscaled results. The validation statistics are listed in Table 3 and show that the downscaling approach greatly increased the r^2 values by 88.1%, 44.5% and 27.2% for events e4, e5 and e6, respectively. For events e1and e2, the r^2 values of the downscaled precipitation decreased slightly but were still at an acceptable level. More importantly, the RMSE and biases for all six events were efficiently reduced after the downscaling process. The RMSE values decreased by 16–64%, and the biases decreased by 54–99%, indicating that both the absolute and relative errors were greatly reduced after being downscaled.

To further evaluate the efficiency of the downscaling approach, it was compared with the conventional spline and kriging interpolation methods. Cross validation of the directly interpolated precipitation fields were conducted, and the results are summarized in Table 4. Except for event e3, the downscaling approach gives better results than the conventional interpolation methods, with several times higher r^2 values and much lower RMSE values.

4. Conclusion and discussion

This study developed a new downscaling approach based on the effects of local environmental factors on the spatial distribution of precipitation. The orographical effect and pre-storm meteorological conditions were examined, and their relationships with precipitation were used in the downscaling scheme. The approach was applied to disaggregate the original $0.25^\circ \times 0.25^\circ$ resolution TRMM 3B42 precipitation data to 1×1 km resolution for six rainstorm events in the Xiao River basin. The validation results show that this approach effectively represents the spatial pattern of the precipitation fields and preserves the rainfall intensity observed at the raingauge stations. It provides high resolution precipitation fields and improves the accuracy of the original TRMM data at the same time. This approach also provides better results than direct interpolation with conventional spline and kriging methods. The main findings in this study and their implications are discussed below.

First, the investigation of the relationships between precipitation and related environmental factors reveals that the pre-storm meteorological conditions play a more important role than the topographical variables in explaining the variation of precipitation in short-term extreme rainfall events. The orographical effect can dominate the accumulated precipitation over relatively long

periods in the mountainous areas but may not in other cases. In addition, the variables relating to the interactions between different elements (for example, aspect angle and topographical roughness) are more effective than variables that only consider characteristics of the pixel (slope aspect and pixel elevation), indicating the complex influence that topography may have on local precipitation.

Second, precipitation generally increases with elevation and decreases with aspect angle due to the topographical lifting effect on airflow, which could intensify the rainfall. Meanwhile, higher temperature and humidity tend to cause more precipitation as a result of more active convective systems and more moisture in the atmosphere. The topographical roughness has a negative impact on precipitation because higher value of roughness indicates more friction between the earth's surface and airflow and higher consumption of water vapor from the sea. However, the influence of these environmental factors varied among the different events because each event was caused by distinct and complicated microphysical processes. The proposed approach considers the major aspects of the rainfall formation mechanism but fails to take into account the detailed micro-meteorological information due to data limitations.

Third, among the six events, event e3 acted as an outlier and had the poorest downscaling performance. Closer inspection of event e3 revealed that it had different formation mechanism from the other events. The other rainfall events were caused by strong convective systems with water vapor coming from the southeast, and precipitation tended to be more intense in the south (see Fig. 5a). However, event e3 was controlled by an upper-level southern branch trough and was affected by weak cold surface air, and the rainfall was heavier in the northwest (see Fig. 5b). The distinct mechanism of event e3 was responsible for the failure of the downscaling approach because the approach is designed for extreme convective rainfall events in which the orographical effect and pre-storm meteorological conditions play important roles. This demonstrates the need for careful diagnosis of the micro-meteorological background before implementing the method. Further study is required to extend the method to other types of rainfall events.

Overall, two main sources concerning the imperfection of data and model contribute to the notable uncertainties in the final results. Subject to the accuracy of the sensors and derivation algorithms, currently available satellite-based precipitation products do not match well with actual observations (see Table 3). TRMM 3B42 tends to underestimate the precipitation from low clouds and high but relatively thin clouds that are at low temperatures [26]. This factor accounts for the majority of the uncertainties in the final results. However, the anticipated Global Precipitation Measurement (GPM) mission [27] is designed to provide precipitation data with high temporal/spatial resolution and reduced uncertainty [28]. It is expected that the bias from the remote sensing measurements of precipitation could greatly decrease in the future.

With regards to the downscaling model, the first important issue is the scale-independent characteristic of the multivariate relationships between precipitation and environmental factors, which lays the foundation of this study. It is reasonable to question this assumption and ask a more profound investigation, because the orographical effect in the model may vary among different scales, providing detailed information or being smoothed with fine and coarse resolution respectively. However, we believe that the difference in the multivariate relationships derived at different scales may not be significant. Subject to the property of spatial autocorrelation, the orographical effect may not change too much when the resolution range does not exceed a certain threshold in the downscaling process. Mass et al. reviewed and extended the study about the benefits of increasing resolution in numerical weather forecasting and concluded that decreasing resolution to less than 10–15 km generally improves the realism of the results but does not necessarily significantly improve the accuracy of the forecasts [29].We also have found some evidence from other studies that are

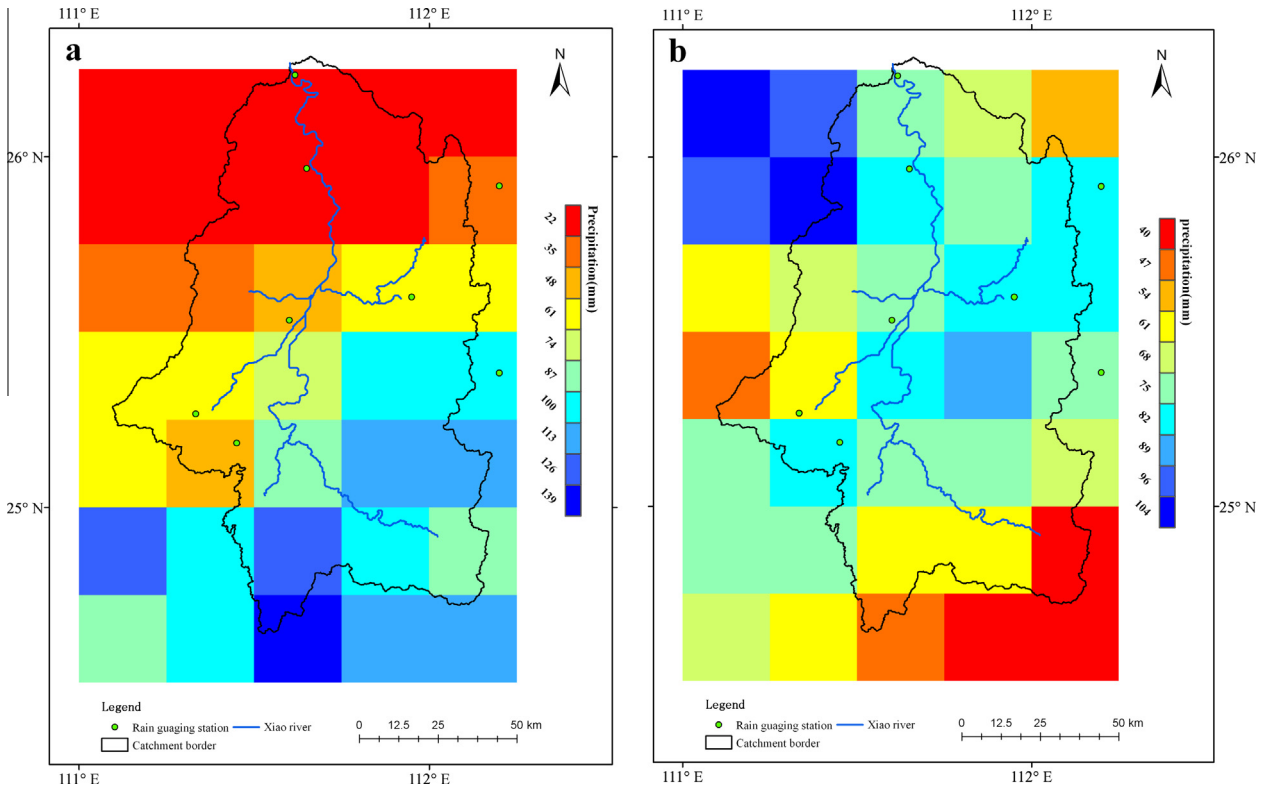

Fig. 5. Comparison of the original TRMM 3B42 precipitation field for events e1 (a) and e3 (b).

supportive of our assumption [30,31]. Therefore it is appropriate to assume the impacts of environmental factors on precipitation to be stationary and establish the downscaling model.

In addition, as the interaction between airflow and topography is implicit and hard to be fully quantified and the physical mechanisms that govern the rainfall variability at different scales have not been well investigated [22], the estimated multivariate regression relationships among precipitation, topography and meteorological conditions only reflect part of the environmental impacts on precipitation and also cause some of the uncertainty. Future studies should emphasize the microphysical processes of extreme rainfall events with more rigorous assessments of the meteorological conditions and their interaction with the surface and incorporate all of the important elements in the downscaling scheme.

Rainfall is a governing factor in the entire hydrologic cycle and greatly influences runoff generation and soil moisture dynamics. Accurate measurement of precipitation at fine spatial and temporal scales is of key importance for the improvement of our ability to simulate land surface hydrological processes and predict hydrometeorological hazards, such as floods and droughts. The proposed downscaling approach is promising for applications of extreme rainfall event management because it well captures the spatial variation of precipitation and closes the gap in scale between satellite precipitation data and model requirements. With improvement of satellite-based precipitation products, more accurate precipitation fields with high resolution can be expected from the downscaling approach, and it will be useful in practical operational systems for the assessment and prediction of extreme rainfall events.

Acknowledgments

This work was supported by the 973 project "Adaptation Paradigms to Global and China's Environmental Risks" under Grant 2012CB955404, Ministry of Science and Technology of China and 111 project "Hazard and Risk Science Base at Beijing Normal University" under Grant B08008, Ministry of Education and State Administration of Foreign Experts Affairs, People's Republic of China. Meanwhile, the authors would like to thank the Editor and anonymous reviewers for their constructive comments and remarks.

References

[1] Field CB, Barros V, Stocker TF, Qin D, Dokken DJ, Ebi KL. Managing the risks of extreme events and disasters to advance climate change adaptation. In: A special report of working groups I and II of the intergovernmental panel on climate change. Cambridge University Press; 2012. <http://ipcc-wg2.gov/SREX/>.

[2] Peterson TC, Stott PA, Herring S. Explaining extreme events of 2011 from a climate perspective. Bull Am Meteorol Soc 2012;93:1041–67. http://dx.doi.org/10.1175/bams-d-12-00021.1.

[3] Min S-K, Zhang X, Zwiers FW, Hegerl GC. Human contribution to more-intense precipitation extremes. Nature 2011;470:378–81. http://dx.doi.org/10.1038/nature09763.

[4] Alexander LV, Zhang X, Peterson TC, Caesar J, Gleason B, Klein Tank AMG, et al. Global observed changes in daily climate extremes of temperature and precipitation. J Geophys Res 2006;111:D05109. http://dx.doi.org/10.1029/2005jd006290.

[5] DFO. Dartmouth Flood Observatory; 2012. <http://www.dartmouth.edu/~floods/>.

[6] Karl TR, Easterling DR. Climate extremes: selected review and future research directions. Clim Change 1999;42:309–25. http://dx.doi.org/10.1023/a:1005436904097.

[7] Guo J, Liang X, Ruby Leung L. Impacts of different precipitation data sources on water budgets. J Hydrol 2004;298:311–34. http://dx.doi.org/10.1016/j.jhydrol.2003.08.020.

[8] Adler RF, Huffman GJ, Chang A, Ferraro R, Xie P-P, Janowiak J, et al. The version-2 global precipitation climatology project (GPCP) monthly precipitation analysis (1979–Present). J Hydrometeorol 2003;4:1147–67. http://dx.doi.org/10.1175/1525-7541(2003)004<1147:tvgpcp>2.0.co;2.

[9] Sorooshian S, Hsu KL, Gao X, Gupta HV, Imam B, Braithwaite D. Evaluation of PERSIANN system satellite-based estimates of tropical rainfall. Bull Am Meteorol Soc 2000;81:2035–46. http://dx.doi.org/10.1175/1520-0477(2000)081<2035:eopsse>2.3.co;2.

[10] Huffman GJ, Bolvin DT, Nelkin EJ, Wolff DB, Adler RF, Gu G, et al. The TRMM multisatellite precipitation analysis (TMPA): quasi-global, multiyear, combined-sensor precipitation estimates at fine scales. J Hydrometeorol 2007;8:38–55. http://dx.doi.org/10.1175/jhm560.1.

[11] Su F, Hong Y, Lettenmaier DP. Evaluation of TRMM multisatellite precipitation analysis (TMPA) and its utility in hydrologic prediction in the La Plata basin. J Hydrometeorol 2008;9:622–40. http://dx.doi.org/10.1175/2007jhm944.1.

[12] Gebremichael M, Krajewski WF, Over TM, Takayabu YN, Arkin P, Katayama M. Scaling of tropical rainfall as observed by TRMM precipitation radar. Atmos Res 2008;88:337–54. http://dx.doi.org/10.1016/j.atmosres.2007.11.028.

[13] Rahman S, Bagtzoglou AC, Hossain F, Tang L, Yarbrough LD, Easson G. Investigating spatial downscaling of satellite rainfall data for streamflow simulation in a medium-sized basin. J Hydrometeorol 2009;10:1063–79. http://dx.doi.org/10.1175/2009jhm1072.1.

[14] Prudhomme C, Reed DW. Mapping extreme rainfall in a mountainous region using geostatistical techniques: a case study in Scotland. Int J Climatol 1999;19:1337–56. http://dx.doi.org/10.1002/(sici)1097-0088(199910)19:12<1337::aid-joc421>3.3.co;2-7.

[15] Jia S, Zhu W, Lű A, Yan T. A statistical spatial downscaling algorithm of TRMM precipitation based on NDVI and DEM in the Qaidam Basin of China. Remote Sens Environ 2011;115:3069–79. http://dx.doi.org/10.1016/j.rse.2011.06.009.

[16] Gottardi F, Obled C, Gailhard J, Paquet E. Statistical reanalysis of precipitation fields based on ground network data and weather patterns: application over French mountains. J Hydrol 2012;432–433:154–67. http://dx.doi.org/10.1016/j.jhydrol.2012.02.014.

[17] Pavlopoulos H. A stochastic framework for downscaling processes of spatial averages based on the property of spectral multiscaling and its statistical diagnosis on spatio-temporal rainfall fields. Adv Water Resour 2011;34:990–1011. http://dx.doi.org/10.1016/j.advwatres.2011.05.006.

[18] Perica S. Model for multiscale disaggregation of spatial rainfall based on coupling meteorological and scaling descriptions. J Geog Res 1996;101:26347–61. http://dx.doi.org/10.1029/96JD01870.

[19] Ahrens B. Rainfall downscaling in an alpine watershed applying a multiresolution approach. J Geophys Res 2003;108:8388. http://dx.doi.org/10.1029/2001jd001485.

[20] Deidda R. Rainfall downscaling in a space–time multifractal framework. Water Resour Res 2000;36:1779–94. http://dx.doi.org/10.1029/2000wr900038.

[21] Tao K, Barros AP. Using fractal downscaling of satellite precipitation products for hydrometeorological applications. J Atmos Oceanic Technol 2010;27:409–27. http://dx.doi.org/10.1175/2009jtecha1219.1.

[22] Bindlish R, Barros AP. Disaggregation of rainfall for one-way coupling of atmospheric and hydrological models in regions of complex terrain. Global Planet Change 2000;25:111–32. http://dx.doi.org/10.1016/S0921-8181(00)00024-2.

[23] Sobel AH, Nilsson J, Polvani LM. The weak temperature gradient approximation and balanced tropical moisture waves. J Atmos Sci 2001;58:3650–65. http://dx.doi.org/10.1175/1520-0469(2001)058<3650:twtgaa>2.0.co;2.

[24] Sawunyama T, Hughes DA. Application of satellite-derived rainfall estimates to extend water resource simulation modelling in South Africa. Water SA 2008;34:1–9. <http://eprints.ru.ac.za/999/1/Application.pdf>.

[25] Prudhomme C, Reed DW. Relationships between extreme daily precipitation and topography in a mountainous region: a case study in Scotland. Int J Climatol 1998;18:1439–53. http://dx.doi.org/10.1002/(SICI)1097-0088(19981115)18:13<1439::AID-JOC320>3.0.CO;2-7.

[26] Ward E, Buytaert W, Peaver L, Wheater H. Evaluation of precipitation products over complex mountainous terrain: a water resources perspective. Adv Water Resour 2011;34:1222–31. http://dx.doi.org/10.1016/j.advwatres.2011.05.007.

[27] Smith E, Asrar G, Furuhama Y, Ginati A, Mugnai A, Nakamura K, et al. International global precipitation measurement (GPM) program and mission: an overview. In: Levizzani V, Bauer P, Turk FJ, editors. Measuring precipitation from space. Netherlands: Springer; 2007. p. 611–53. http://dx.doi.org/10.1007/978-1-4020-5835-6_48.

[28] Tian Y, Peters-Lidard CD, Choudhury BJ, Garcia M. Multitemporal analysis of TRMM-based satellite precipitation products for land data assimilation applications. J Hydrometeorol 2007;8:1165–83. http://dx.doi.org/10.1175/2007jhm859.1.

[29] Mass CF, Ovens D, Westrick K, Colle BA. Does increasing horizontal resolution produce more skillful forecasts? Bull Am Meteorol Soc 2002;83:407–30. http://dx.doi.org/10.1175/1520-0477(2002)083<0407:dihrpm>2.3.co;2.

[30] Brooks HE, Doswell CA, Maddox RA. On the use of mesoscale and cloud-scale models in operational forecasting. Weather Forecasting 1992;7:120–32. http://dx.doi.org/10.1175/1520-0434(1992)007<0120:otuoma>2.0.co;2.

[31] Buzzi A, Foschini L. Mesoscale meteorological features associated with heavy precipitation in the southern alpine region. Meteorol Atmos Phys 2000;72:131–46. http://dx.doi.org/10.1007/s007030050011.